

Shaping Spectral Leakage for IEEE 802.11p Vehicular Communications

Thinh H. Pham^{*}, Ian Vince McLoughlin[†], Suhaib A. Fahmy^{*}

^{*}School of Computer Engineering

Nanyang Technological University, Singapore

Email: hung3@e.ntu.edu.sg

[†]School of Information Science and Technology

University of Science and Technology of China, Hefei, China

Abstract—IEEE 802.11p is a recently defined standard for the physical (PHY) and medium access control (MAC) layers for Dedicated Short-Range Communications. Four Spectrum Emission Masks (SEMs) are specified in 802.11p that are much more stringent than those for current 802.11 systems. In addition, the guard interval in 802.11p has been lengthened by reducing the bandwidth to support vehicular communication (VC) channels, and this results in a narrowing of the frequency guard. This raises a significant challenge for filtering the spectrum of 802.11p signals to meet the specifications of the SEMs. We investigate state of the art pulse shaping and filtering techniques for 802.11p, before proposing a new method of shaping the 802.11p spectral leakage to meet the most stringent, class D, SEM specification. The proposed method, performed at baseband to relax the strict constraints of the radio frequency (RF) front-end, allows 802.11p systems to be implemented using commercial off-the-shelf (COTS) 802.11a RF hardware, resulting in reduced total system cost.

I. INTRODUCTION

Dedicated Short-Range Communications (DSRC) refers to the provision of a wireless channel for new vehicular safety applications through vehicle-to-vehicle (V2V) and Road to Vehicle (RTV) communications. In 2010 the IEEE defined a standard for DSRC's PHY and MAC layers [1], named IEEE 802.11p. The PHY in 802.11p is largely inherited from the well-established IEEE 802.11a OFDM PHY, with several changes aimed at improving performance in vehicular environments. The advantage of building on 802.11a is a significant reduction in the cost and development effort necessary to develop 802.11p hardware and software. It also plays an important role in allowing backwards compatibility from 802.11p to 802.11a [2], [3].

Essentially, three changes are made in IEEE 802.11p [4]: First, 802.11p defines a 10 MHz channel width instead of the 20 MHz used by 802.11a. This extends the guard interval to address the effects of Doppler spread and inter-symbol interference in a VC channel. Secondly, 802.11p defines several improvements in receiver adjacent channel rejection performance to reduce the effect of cross channel interference that is especially important in vehicle communication channels. Finally, 802.11p defines four spectral emission masks (SEMs) corresponding to class A to D operations that are specified and issued in FCC CFR47 Sections 90.377 and 95.1509. These

are more stringent than for current 802.11 radios, in order to improve performance in urban vehicle scenarios.

Thanks to the similarities between the two PHYs, some work has focused on making 802.11a PHY devices compatible with 802.11p [5], [6], [2]. Most researchers deal with the transformation in four parts, namely, reducing channel bandwidth, channel estimation, transmission power requirements, and effective channel access performance. Due to a dearth of affordable 802.11p prototype hardware, existing wireless testbeds for 802.11p tend to use modified commercial off-the-shelf (COTS) 802.11a hardware [5]. For example, Almeda and Matos present a front-end using 802.11a hardware that is targeted to comply with the specification of 802.11p [7]. Despite strict constraints, it still does not meet the SEM requirement. Fuxjäger et al. present an implementation of a fully functional 802.11p transmitter using GNU Radio, a software-defined radio platform [8]. However, the output signal spectrum contains two peaks caused by image frequencies, which the output filter is unable to remove. Hence, it does not even satisfy class A. Contrast this to an early prototype transceiver, based on a modified Atheros chip set [8], which fulfils class A requirements, but can not meet class C specifications. The consequence of the stringent SEMs significantly increases the difficulty, and hence cost, of implementing new silicon or hardware for 802.11p. To the best of the authors' knowledge, there are no published implementations or testbeds for 802.11p that are able to meet the class D specifications. There remains a debate regarding whether and when chip makers will be able to meet such requirements [4].

To relax the stringent specification of the SEMs, additional signal processing at baseband is investigated in this paper for spectral leakage filtering of the 802.11p OFDM signal. Increasing processing at baseband to address this challenge is a sensible approach as much of the baseband processing is done on optimised processors or FPGAs [9], where the relative increase in computational cost can be easily tolerated. In particular, this paper contributes a new method for filtering the OFDM signal at baseband in an effort to fulfil the stringent class D specifications of the IEEE 802.11p standard.

II. SIGNAL MODEL

We consider an 802.11p OFDM symbol to have inverse fast Fourier transform (IFFT) length and cyclic prefix (CP) length of $N = 64$ and $N_{CP} = 16$, respectively. Therefore, the length of an 802.11p symbol including CP is $N_T = N + N_{CP} = 80$. A sample $x(m)$ of the OFDM symbol ($0 \leq m \leq N_T - 1$) in the time domain can be expressed as

$$x(m) = \frac{1}{N} \sum_{k=0}^{N-1} X(k) e^{i2\pi \frac{k}{N} (m - N_{CP})}, \quad (1)$$

where $X(k)$ is the frequency domain representation of data subcarriers. Typically, the OFDM symbol samples are transmitted sequentially, which is equivalent to multiplying symbols with a rectangular window function, p . The transmitted samples of 802.11p signal can be expressed as;

$$x(n) = \frac{1}{N} \sum_{l=-\infty}^{\infty} \sum_{k=0}^{N-1} X(k) p(n - lN_T) e^{i2\pi \frac{k}{N} (n - N_{CP} - lN_T)} \quad (2)$$

The 802.11p symbol has 16 samples for CP (i.e. the same as in 802.11a). The CP is a guard interval inserted to avoid inter-symbol interference (ISI) when OFDM symbols are transmitted over a delay-dispersive multi-path channel, represented by a channel impulse response (CIR) with length h , derived from the delay spread of the channel. If the CP is shorter than the channel delay, ISI will be present in received symbols. Unfortunately, the 802.11p VC channel tends to experience a larger delay spread than WLAN: according to empirical VC channel models in [10], [11], maximum delay spread varies depending on different propagation models and traffic environment. The RTV model for suburban street, urban canyon, and expressway, have maximum excess delay of 700, 501, and 401 ns, respectively [10]. For the V2V model, measurements in [11] show that delay spread is largest for urban areas and smallest for highway areas. The 90% measured value of delay spread for urban areas is near 600 ns. In 802.11p, guard intervals are lengthened to avoid ISI, but this raises some challenges in the frequency domain. First, reducing bandwidth requires a higher quality factor front-end filter circuit for the higher frequency carrier compared to 802.11a. Second, in an 802.11p system, similar to 802.11a, there are 6 sub-carrier spacings used for the frequency guard per side. But reducing the sampling frequency leads to a narrowing of the frequency guard. Generally, to improve performance in VC channels with large delay spread, the timing guard is increased, narrowing the frequency guard and resulting in more strict filtering constraints.

In addition, 802.11p will operate in the 5.9 GHz DSRC spectrum divided into seven 10 MHz bands. This channelization allows the MAC upper layer, i.e., IEEE 1609.4, to perform multi-channel operations [12]. The mechanism allows safety and other applications to occupy separate channels to reduce interference. The four 802.11p SEMs are defined to reduce the effect of ICI. Wu et al. [13] showed that transmitters on adjacent service channels still cause inter-channel interference

(ICI) in the safety channel, even if they satisfy the class C requirement. Shaping 802.11p spectral leakage is thus potentially important in helping to eliminate ICI.

III. USING PULSE SHAPING FOR 802.11P

Pulse shaping (using a smooth rather than rectangular pulse), recommended in 802.11a, is effective at reducing side lobes, though it can induce distortion in the subcarriers. One way to avoid this is to add extending parts, i.e. CP and a cyclic suffix (CS) before and after each conventional OFDM symbol respectively, and to multiply the extended symbol with a smoothing function. While the CP in conventional OFDM is used as a guard interval, here it is also used for pulse shaping.

Pulse shaping extends the N_T length of the OFDM signal by a roll-off factor, β . The overhead of extending CS results in spectral loss; overlapping of the CP and CS of consecutive symbols shown in Fig. 1 is needed to form a transmitted symbol to reduce this loss, but causes ISI in the overlapped region.

Pulse shaping using the overlapping method is effectively equivalent to shortening the OFDM guard interval. A larger β obtains greater compression in spectral leakage but reduces the effective guard interval. When βN_T is increased to equal the CP length, the effective guard interval is reduced to zero (no guard interval) to prevent channel-induced ISI. Three state-of-the-art smoothing functions for pulse shaping are investigated. The first is present in the IEEE 802.11a standard. The second is based on a raised cosine function proposed by Bala et al. [14]. The last is based on the characteristics of functions with vestigial symmetry presented by Castanheira and Gameiro [15]. The three functions are rewritten in discrete form in Equations (3), (4), (5), respectively.

$$p_1 = \begin{cases} \sin^2(\frac{\pi}{2}(0.5 + \frac{m}{2\beta N_T})), & 0 \leq m < \beta N_T \\ 1, & \beta N_T \leq m < N_T \\ \sin^2(\frac{\pi}{2}(0.5 - \frac{m - N_T}{2\beta N_T})), & N_T \leq m < (1 + \beta)N_T \end{cases} \quad (3)$$

$$p_2 = \begin{cases} \frac{1}{2} + \frac{1}{2} \cos(\pi(1 + \frac{m}{\beta N_T})), & 0 \leq m < \beta N_T \\ 1, & \beta N_T \leq m < N_T \\ \frac{1}{2} + \frac{1}{2} \cos(\pi(1 + \frac{m - N_T}{\beta N_T})), & N_T \leq m < (1 + \beta)N_T \end{cases} \quad (4)$$

$$p_3 = \begin{cases} \frac{1}{2} + \frac{9}{16} \cos(\pi(1 - \frac{m}{\beta N_T})) \\ -\frac{1}{16} \cos(3\pi(1 - \frac{m}{\beta N_T})), & 0 \leq m < \beta N_T \\ 1, & \beta N_T \leq m < N_T \\ \frac{1}{2} + \frac{9}{16} \cos(\pi \frac{m - N_T}{\beta N_T}) \\ -\frac{1}{16} \cos(3\pi \frac{m - N_T}{\beta N_T}), & N_T \leq m < (1 + \beta)N_T \end{cases} \quad (5)$$

The decay of OFDM spectral side lobes using pulse shaping is first investigated by assuming that the effect of image spectrum caused by interpolation or digital-to-analog conversion (DAC) is negligible. This assumption is made because the band gap between 802.11p spectrum and its image spectrum is relatively narrow. The image spectrum can affect the ability to shape spectrum leakage (this is investigated later). Fig. 2 shows simulation results for three smoothing functions with respect to the image spectrum.

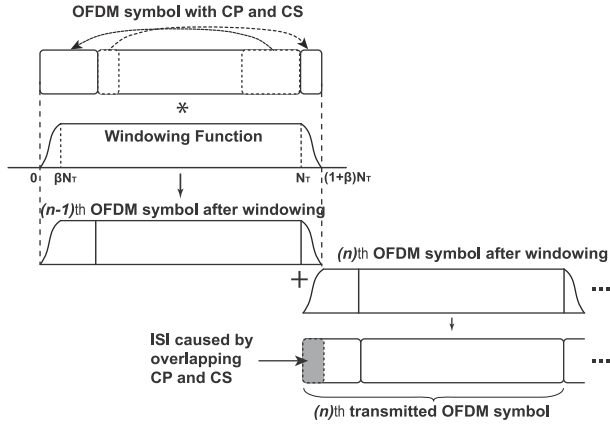


Fig. 1. Pulse Shaping operation performed on OFDM symbols.

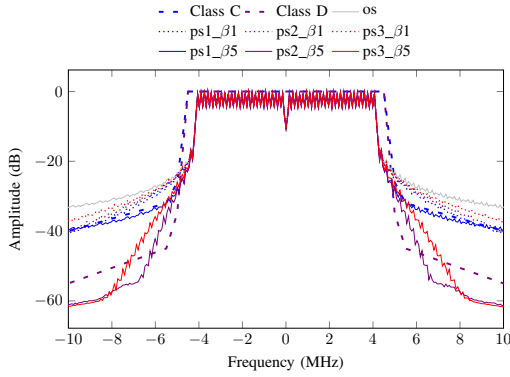


Fig. 2. Spectrum of pulse shaping OFDM symbols using three smoothing functions.

os is the original OFDM spectrum without using pulse shaping. $ps1_beta1$, $ps2_beta1$, $ps3_beta1$ denote the spectrum of the OFDM signal using smoothing functions: $p_1(m)$, $p_2(m)$, $p_3(m)$, respectively with roll-off factors chosen as $\beta N_T = 1$. Similarly, $ps1_beta5$, $ps2_beta5$, $ps3_beta5$ present the spectrum of OFDM signals with $\beta N_T = 5$. In the case of using one guard interval sample, the spectral leakage is reduced compared to the original OFDM signal. $p_1(m)$ obtains better results in comparison to the other two, however, the shaped spectra still do not meet the requirement of class C. When 5 samples of CP are used for pulse shaping, shaping spectrum leakage using $p_2(m)$ and $p_3(m)$ achieves a significant improvement. The spectrum using $p_2(m)$ satisfies class C and almost meets the requirement of class D. Ignoring the presence of an image spectrum, the pulse shaping method can take part of the guard interval for applying the smoothing function in order to shape the spectral leakage and achieve stringent SEM compliance. Fig. 3 shows simulation results for pulse shaping 802.11p OFDM symbols with the presence of the image spectrum.

The spectrum of OFDM signals using pulse shaping in Fig. 3 is almost identical to (but slightly better than) the original OFDM signal. With the presence of an image spectrum, pulse shaping does not obtain significant improvement in terms of limiting the spectrum leakage in 802.11p. The band gap between the main spectrum and the image spectrum is not

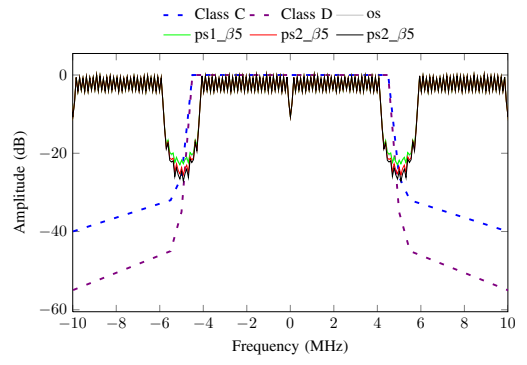


Fig. 3. Spectrum of pulse shaping 802.11p OFDM symbols with the presence of the image spectrum.

large enough for pulse shaping to obtain a significant spectral leakage decay. Hence, this method does not help to cancel the image spectrum caused by interpolation or DAC. The next section investigates applying an FIR filter to cancel the image spectrum.

IV. IMAGE SPECTRUM CANCELLATION BY FIR FILTER

The critical issue for 802.11p signals meeting the stringent requirements of the class D mask is that the frequency guards are narrow and the frequency carrier is relatively high (5.9 GHz) compared to 802.11a. Interpolation can be used at baseband to increase sampling frequency, thereby extending baseband bandwidth. Image spectra are repeats of the original baseband spectrum, present because of interpolation effects. An interpolation filter, commonly implemented as an FIR filter, may be used to cancel image spectra.

On one hand, the narrow band gap between main and adjacent image spectra requires a long impulse response FIR filter. On the other hand, the impulse response of the FIR filter has a similar effect to the impulse response of the overall channel in terms of inducing ISI. The FIR filter reduces the effective guard interval of OFDM symbols [16]. Its design also needs to deal with the tradeoff between the length of filter to avoid ISI and the transition band and attenuation of the filter to meet the requirement of SEMs. We investigate several widely used FIR filters, listed in Table I, as applied to 802.11p. An empirical formula [17] is used to estimate the length of each filter in terms of attenuation A and transition band $\Delta\omega$. The specifications of the class D SEM for 802.11p are used to calculate the required number of taps with L-fold interpolation. The required lengths of these FIR filters for 802.11p are larger than the guard interval of the 802.11p symbol.

To avoid ISI, the maximum length of the FIR filter is derived by taking into account guard interval and CIR. By assuming that the delay spread of the VC channel is constrained to a maximum of 600 ns (see Section 2), CIR is equivalent to 6 samples of the 802.11p guard interval. That assumption is based on the result of the channel model in [10], [11]. Therefore, the effective guard interval remains 10 samples for filtering. In addition, when the filter is used in a transmitter, a matched filter is required at the receiver [16] resulting in 5 samples of guard interval for transmitter filtering. L-fold

TABLE I
POPULAR WINDOW-BASED FIR FILTER LENGTHS

Window	Stopband Atten.	Filter Len.	Length for 802.11p
Hamming	-26.5dB	$N = \frac{6.22\pi}{\Delta\omega}$	$N \approx 31L$
Hanning	-31.5dB	$N = \frac{6.65\pi}{\Delta\omega}$	$N \approx 33L$
Blackman	-42.7dB	$N = \frac{11.1\pi}{\Delta\omega}$	$N \approx 55L$
Kaiser	—	$N = \frac{A-7.95}{2.23\Delta\omega}, A > 21$ $N = \frac{5.79}{\Delta\omega}, A < 21$	$N \approx 33L$
Chebyshev	—	$N = \frac{2.06A-16.5}{2.29\Delta\omega}$	$N \approx 67L$

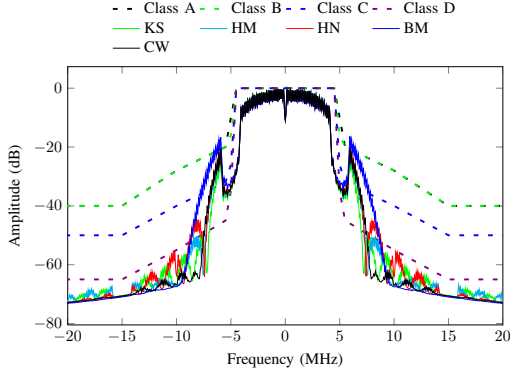


Fig. 4. Spectra of filtered OFDM symbols for 802.11p using different FIR filters.

interpolation is used at the transmitter. Therefore, the permitted length of the FIR filters is $5 \times L$, and that is applied to design the FIR filters. A simulation is performed with $L = 8$ to evaluate filtered spectra for the 802.11p signal. These FIR filters are employed to filter the interpolated OFDM signal, and the results of the filtered spectra are presented in Fig. 4.

KS, *HM*, *HN*, *BM*, *CW* denote the filtered spectra obtained by using Kaiser, Hamming, Hanning, Blackman, Chebyshev windows, respectively. Applying the filters causes two wide auxiliary peaks beside the main spectrum. The Blackman window filtered spectrum slightly exceeds the requirement of class A. That of the remaining window filters does meet the requirements of classes A and B but not of classes C and D. Hence, given the effective guard interval of 802.11p, FIR filtering does not provide a solution.

V. PROPOSED METHOD

This section proposes a novel method for achieving the class D specification. The proposed method relies upon spectrum manipulation, using the extending frequency guard technique, allied with pulse shaping and an FIR filter. It is performed in a specified procedure with the following steps: first, the frequency guard is extended [16] by increasing the size of the IFFT to M times the original IFFT. The sampling frequency is also increased M times to maintain the same subcarrier spacing. The data symbols employ lower sub-carriers that are the same as those in the original IFFT. The remaining sub-carriers are zero-padded, resulting in extending the frequency guard. Second, pulse shaping is employed to shape the spectral

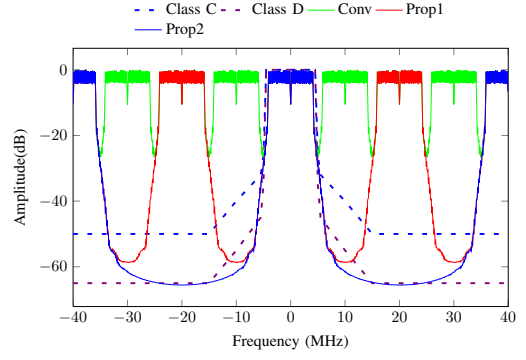


Fig. 5. Spectrum of 802.11p signal of the proposed method after interpolation.

leakage to meet the specification of class D. Third, L -fold interpolation is performed to extend the baseband spectrum and hence relax the requirement of the RF front-end hardware. Finally, thanks to the extended frequency guard, a short length FIR filter can easily filter out the final image spectrum caused by interpolation.

Continuing the assumption from Section IV, the CIR length does not exceed 600 ns. Therefore, the effective guard interval which is equivalent to the length of 10 samples of the original CP, i.e., $10 \times 100 = 1000$ ns is used for the pulse shaping and FIR filter. By choosing an DAC sampling frequency of 80 MHz, the sampling frequency of 802.11p is increased by 8 times compared to the original (10 MHz). Two options denoted as *Prop1*, *Prop2* are studied. *Prop1* doubles the size of IFFT, i.e., $M = 2$, this means doubling the sampling frequency, to extend the frequency guard. Then 4-fold interpolation, i.e., $L = 4$, is required to obtain a sampling frequency of 80 MHz. *Prop2* quadruples the size of IFFT, i.e., $M = 4$; Then 2-fold interpolation, i.e., $L = 2$, is performed to maintain the sampling frequency at 80 MHz. Based on the results in section III, $p_2(m)$ is employed with $\beta N_T = 5 \times M$, that is equivalent to the length of 5 samples of the original CP, i.e., 500 ns. It should be noted that after extending the frequency guard, the number of samples in the symbol including CP, is increased M times. Fig. 5 shows the shaped spectrum of the proposed method after interpolation in the baseband, at 80 MHz. The result is also compared to the original spectrum denoted *Conv*, and the specifications of classes C and D. The main spectrum of *Prop1*, *Prop2* almost satisfy class D. The image spectrum of *Prop1* is present at ± 40 MHz and ± 20 MHz whilst *Prop2* has an image spectrum at ± 40 MHz.

A simple short length FIR filter is needed to cancel the image spectra. The remaining guard interval for the transmitter filter and matched filter is 500 ns. Therefore, the maximum impulse response of the FIR filter is 250 ns, which is equivalent to $2.5 \times M \times L$ samples at the 80 MHz sampling frequency.

FIR filters are designed for *Prop1*, *Prop2* using a Kaiser window. Because the frequency guard of *Prop1* is still relatively narrow, it requires an FIR filter with the length of 20 samples to cancel the image spectrum. Fig. 6 shows the result of spectrum filtering for *Prop1* in comparison to the original

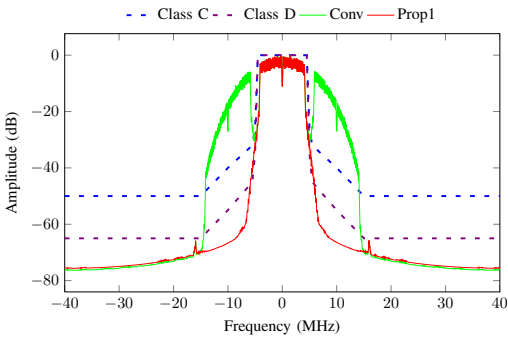


Fig. 6. Filtered Spectrum of 802.11p signal using option *Prop1*.

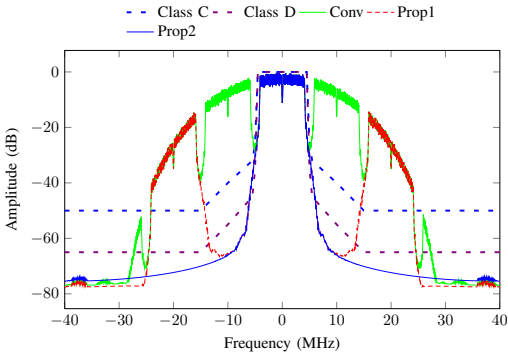


Fig. 7. Filtered Spectrum of 802.11p signal using option *Prop2*.

OFDM spectrum and class C, D SEMs. As can be seen in the *Prop1* spectrum, there are still two small peaks caused by the image spectrum. These peaks are compressed by the FIR filter to meet the class D requirement. Slight distortion is present in the main spectrum because of the effect of the FIR filter. *Prop2* has a wider frequency guard compared to *Prop1*. The FIR filter only requires a length of 12 samples to cancel the image spectrum and the remaining effective guard interval of 200 ns is reserved. Fig. 7 shows the result of spectral filtering for *Prop2* and *Prop1* with respect to the class C and D SEMs. The image spectrum of *Prop2* can be cancelled by a short length FIR filter whilst the image spectrum of *Prop1* still remains larger in magnitude. Hence, *Prop2* meets the class D specification.

The simulation results demonstrate that the proposed technique for shaping spectral leakage can meet the specification of class D, the most stringent of the four 802.11p SEMs. *Prop2* obtains better performance in terms of distortion and effective guard interval compared to *Prop1*, but pays the cost of a higher computational requirement due to the increased IFFT size. It should be noted that the additional computation needed for signal processing in the baseband (which contains low cost, power components), can be repaid by relaxing the specification of the RF front-end design (which tends to require more costly, and higher power components).

VI. CONCLUSION

This paper has investigated the shaping of leakage spectrum for 802.11p at the baseband. The narrow frequency guard

defined in 802.11p does not allow common pulse shaping techniques to perform well, ruling out many methods developed for 802.11a. The 802.11p guard interval is not long enough for an FIR filter to perfectly cancel the image spectrum caused by interpolation or the DAC process. A new leakage spectrum shaping method was proposed for 802.11p systems. It entails performing filtering based upon the extending the frequency guard, allied with careful pulse shaping, and simple (much shorter) FIR filtering. Simulations show that the proposed method can meet the specification of class D, the most stringent of the four 802.11p SEMs.

REFERENCES

- [1] *IEEE 802 Standard; Part 11; Amendment 6: Wireless Access in Vehicular Environments*, IEEE std. 802.11p, Jul. 2010.
- [2] W. Vandenberghe, I. Moerman, and P. Demeester, "Approximation of the IEEE 802.11p standard using commercial off-the-shelf IEEE 802.11a hardware," in *International Conference on ITS Telecommunications (ITST)*, 2011, pp. 21–26.
- [3] J. Fernandez, K. Borries, L. Cheng, B. Kumar, D. Stancil, and F. Bai, "Performance of the 802.11p Physical Layer in Vehicle-to-Vehicle Environments," *IEEE Transactions on Vehicular Technology*, vol. 61, no. 1, pp. 3–14, 2012.
- [4] D. Jiang and L. Delgrossi, "IEEE 802.11p: Towards an International Standard for Wireless Access in Vehicular Environments," in *IEEE Vehicular Technology Conference (VTC)*, 2008, pp. 2036–2040.
- [5] D. Lo Iacono and T. Cupaiuolo, "Power Efficient SDR Implementation of IEEE 802.11a/p Physical Layer," *Journal of Signal Processing Systems*, vol. 73, no. 3, pp. 281–289, 2013.
- [6] W.-Y. Lin, M.-W. Li, K.-C. Lan, and C.-H. Hsu, "A Comparison of 802.11a and 802.11p for V-to-I Communication: A Measurement Study," in *Quality, Reliability, Security and Robustness in Heterogeneous Networks*. Springer, 2012, vol. 74, pp. 559–570.
- [7] N. de Almeida, J. Matos, and J. Lopes, "A front end to vehicular communications," in *IEEE International Conference on Computer as a Tool (EUROCON)*, 2011, pp. 1–4.
- [8] P. Fuxjäger, A. Costantini, D. Valerio, P. Castiglione, G. Zacheo, T. Zemen, and F. Ricciato, "IEEE 802.11 p transmission using GNURadio," in *Proceedings of the Karlsruhe Workshop on Software Radios (WSR)*, 2010, pp. 83–86.
- [9] J. Lotze, S. A. Fahmy, J. Noguera, B. Ozgöl, L. Doyle, and R. Esser, "Development framework for implementing FPGA-based cognitive network nodes," in *Proceedings of the IEEE Global Communications Conference (GLOBECOM)*, 2009.
- [10] G. Acosta-Marum and M.-A. Ingram, "Six time and frequency selective empirical channel models for vehicular wireless LANs," *IEEE Vehicular Technology Magazine*, vol. 2, no. 4, pp. 4–11, 2007.
- [11] I. Sen and D. Matolak, "Vehicle - Vehicle Channel Models for the 5-GHz Band," *IEEE Transactions on Intelligent Transportation Systems*, vol. 9, no. 2, pp. 235–245, 2008.
- [12] *IEEE Standard for Wireless Access in Vehicular Environments-Multi-Channel Operations*, IEEE Std 1609.4-2010, Dec. 2010.
- [13] X. Wu, S. Subramanian, R. Guha, R. White, J. Li, K. Lu, A. Bucceri, and T. Zhang, "Vehicular Communications Using DSRC: Challenges, Enhancements, and Evolution," *IEEE Journal on Selected Areas in Communications*, vol. 31, no. 9, pp. 399–408, 2013.
- [14] E. Bala, J. Li, and R. Yang, "Shaping Spectral Leakage: A Novel Low-Complexity Transceiver Architecture for Cognitive Radio," *IEEE Vehicular Technology Magazine*, vol. 8, no. 3, pp. 38–46, 2013.
- [15] D. Castanheira and A. Gameiro, "Novel Windowing Scheme for Cognitive OFDM Systems," *IEEE Wireless Communications Letters*, vol. 2, no. 3, pp. 251–254, 2013.
- [16] B. Farhang-Boroujeny, *Signal Processing Techniques for Software Radios*. Lulu Publishing House, 2008.
- [17] R. J. Kapadia, *Digital Filters Theory, Application and Design of Modern Filters*. Wiley VCH, 2012.